# Hydrogen Production Characteristic of Diesel Reforming under Ship SOFC-GT Operation Environment[#]

Xicong Mi[1], Xusheng Wang[2], Catalina Spataru[3], Xiaojing Lv[1*], Yiwu Weng[1,2*]

1 China-UK Low Carbon College, Shanghai Jiao Tong University, Shanghai, Pudong New Area,201306

2 School of Mechanical Engineering, Shanghai Jiao Tong University, Shanghai, Minhang District, 200240

3 UCL Energy Institute, University College London, Central House | 14 Upper Woburn Place London | WC1H 0NN, United Kingdom

| R | Universal constant of gases (J mol$^{-1}$ K$^{-1}$) |
|---|---|
| T | Temperature (K) |
| P | Pressure (bar) |
| $a_{ji}$ | Atomic number of element j in the i-th component molecule |
| $b_j$ | The amount of the j element |

## ABSTRACT

SOFC/GT hybrid system is proposed as one of the advanced power systems of future ships due to its high efficiency, low emission and fuel flexibility. However, how to efficiently reform marine diesel into $H_2$ is the key to maintaining the operation of SOFC/GT. This paper studies the influence of operating parameters such as S/C, temperature and pressure of ship SOFC/GT hybrid system on $H_2$ production characteristics of marine diesel reforming through numerical simulation and experimental analysis. The results show that under the variable working conditions, the $H_2$ production increases with temperature and the carbon deposition decreases. The increase of S/C promotes the increase of $H_2$ yield and inhibits carbon deposition. Pressure has a negative effect on $H_2$ production. The research results can provide basic technical support for the safe and efficient operation of the SOFC-GT hybrid power system on ships and the continuous supply of fuel.

**Keywords:** marine diesel; ship SOFC-GT; reforming characteristic; $H_2$ yield; carbon deposition

## NONMENCLATURE

| *Abbreviations* | |
|---|---|
| SOFC/GT | Solid Oxide Fuel Cell-Gas Turbine |
| S/C | Steam to Carbon ratio |
| *Symbols* | |
| ΔH | Enthalpy change of reaction (kJ mol$^{-1}$) |
| min.G | Minimum Gibbs free energy (J mol$^{-1}$) |
| $n_i$ | The amount of substance of component i (J mol$^{-1}$) |
| $\overline{g_1}$ | Gibbs free energy of component i in the mixed system (J mol$^{-1}$) |
| $y_i$ | Mole fraction of component i |

## 1. INTRODUCTION

The international shipping industry is developing towards a high-efficiency, low-carbon and clean direction. The ship's power system is the "heart" of the ship, and its performance directly affects a series of indicators such as the ship's rapidity, speed adaptability, endurance, and economy. Therefore, with the increasingly serious problems of energy shortage and environmental pollution, the development of a power system for future green ships is a key issue that needs to be solved urgently in the current shipping field[1-4]. SOFC-GT hybrid system has the advantages of high efficiency (up to 70% or more) and near-zero $NO_X$ emissions. When used as a ship power system, it can not only greatly improve its endurance by 30%, but also reduce oil load, the interference of thermal signal and sound wave signal. So it is one of the most influential ship power technologies being actively developed by countries in the world[5-7].

When SOFC-GT is used on ships, fuel is needed to provide $H_2$, and diesel is the most widely used fuel for ships today. In order to reduce the cost of engineering facility renovation caused by changing fuel, $H_2$ production from diesel reforming can be directly applied to SOFC-GT ships. The safe and efficient operation of the SOFC/GT hybrid system has strict requirements on the distribution of reformed products and the $H_2$ yield of the reformer. At the same time, parameters such as

reforming temperature, pressure, and S/C also need to be well adapted to the power system. Therefore, how to find the best reforming $H_2$ production law and characteristics under the operating environment parameters of ship SOFC/GT hybrid system is the feature and challenge for the current research. The U.S. Office of Naval Research (DOD ONR) conducted the evaluation and development of high-temperature fuel cell/gas turbine hybrid systems based on diesel reforming technology from 2000 to 2011. The results showed that the high-temperature fuel cell efficiency in the hybrid power system could reach 50%, and the overall power generation efficiency could reach more than 65%. It was also pointed out that diesel fuel reforming was the key to efficient operation of fuel cells in hybrid systems[8]. Sun[9] et al. compared a diesel-fueled SOFC-GT hybrid system, a diesel engine, and a gas turbine using a military marine vessel as a platform. Studies had shown that the SOFC-GT hybrid system could save 20-50% of fuel and basically had no NOx emissions. The $H_2$-rich fuel from diesel reforming was very important. Gerardo[10] et al. modeled and simulated the AGR (anode off-gas recirculation) diesel pre-reforming SOFC system, and used it in the APU(auxiliary power unit) for offshore applications to prove its feasibility. Sohyun [11] et al. presented a comprehensive model of diesel ATR(autothermal reforming) over nickel-based catalysts. Simulation results show that diesel reforming efficiency is very sensitive to input variables and temperature. Remzi[12,13] et al. conducted ATR experiments to study the fuel conversion rate and CO concentration at the outlet of a 28kW fuel processor for an integrated fuel cell system, and obtained the optimal parameter set for load changes during steady-state and transient operation.

At present, the research on diesel reforming in the power system is not complete, and the influence mechanism of temperature matching, carbon deposition phenomenon and product distribution needs to be further studied. In this paper, a diesel reforming thermodynamic model will be established based on the Gibbs free energy minimization principle of heterogeneous chemical reactions and compared with the experimental test results. Influence characteristics and parameter adjustment law of the operating environmental parameters of the ship SOFC-GT hybrid system, such as temperature, S/C, and pressure, on distribution of marine diesel reformate are researched The research results can provide basic technical support for the application of diesel-fueled SOFC-GT hybrid system on ships.

## 2. MATHEMATICAL MODEL OF MARINE DIESEL REFORMING

### 2.1 Marine diesel cracking gas reforming reaction system

Marine diesel reforming is divided into three methods: steam reforming (SR), partial oxidation reforming (POR), and autothermal reforming (ATR). Diesel steam reforming has a high $H_2$ yield and is the most widely used. Partial oxidation reforming is an exothermic reaction with fast start-up, but it is difficult to control. Autothermal reforming is a combination of steam reforming and partial oxidative reforming. This paper mainly focuses on the research of diesel steam reforming.

As a complex hydrocarbon, diesel is composed of a variety of large carbon molecules. It can be seen from the experiment that the composition of the cracked gas produced by diesel cracking is small molecular hydrocarbons of $C_1$~$C_5$. The reforming reactions and side reactions considered in this paper are shown in Table 1

Table 1 Reaction of Diesel Cracking Gas Reforming for $H_2$ Production

| Reaction type | Reaction formula | $\triangle H$(kJ/mol) | Reaction Number |
|---|---|---|---|
| Steam reforming | $CH_4+H_2O \leftrightarrow CO+3H_2$ | +205.9 | R1 |
| | $C_2H_4+2H_2O \leftrightarrow 2CO+4H_2$ | +210.2 | R2 |
| | $C_2H_6+2H_2O \leftrightarrow 2CO+5H_2$ | +347.3 | R3 |
| | $C_3H_6+3H_2O \leftrightarrow 3CO+6H_2$ | +373.5 | R4 |
| | $C_3H_8+3H_2O \leftrightarrow 3CO+7H_2$ | +497.7 | R5 |
| | $C_4H_8+4H_2O \leftrightarrow 4CO+8H_2$ | +525.6 | R6 |
| Water gas shift reaction | $CO+H_2O \leftrightarrow CO_2+H_2$ | -41.17 | R7 |
| Methanation reaction | $CO+3H_2 \leftrightarrow CH_4+H_2O$ | -205.9 | R8 |
| Carbon deposition reaction | $CH_4 \leftrightarrow C+2H_2$ | +74.9 | R9 |
| | $CO+H_2 \leftrightarrow C+H_2O$ | -131.3 | R10 |
| | $CO_2+2H_2 \leftrightarrow C+2H_2O$ | -90.1 | R11 |
| | $2CO \leftrightarrow C+CO_2$ | -172.5 | R12 |

## 2.2 Construction of reforming thermodynamic chemical model

Thermodynamic equilibrium analysis was carried out on the weight system of diesel cracking gas, and the specific components were derived from diesel cracking experiments. Because reforming of diesel cracking gas is a multicomponent system, in order to solve the stability, this paper adopts the principle of Gibbs free energy minimum method to solve the components of the equilibrium system.

$$min.\,G = \sum_{i=1}^{N} n_i \bar{g_i} = \sum_{i=1}^{N} n_i g_i^0 + RT \sum n_i \, ln \frac{y_i P}{P_0} \quad (1)$$

Among them, $min.\,G$ is the minimum value of the total Gibbs free energy of the reaction system; $N$ is the number of components in the reaction system; $n_i$ is the amount of substance of the $i$-th component; $\bar{g_i}$ is its Gibbs free energy in the mixed system; $g_i^0$ is its standard Gibbs free energy; $y_i$ is its mole fraction; $P$ is the total reaction pressure; $P_0$ is the atmospheric pressure. When solving the minimization of Gibbs free energy, the following constraints need to be satisfied:

$$n_i \geq 0 \quad (2)$$
$$\sum_i^N n_i a_{ji} = b_j \,(j = 1,2\,...,e) \quad (3)$$

$a_{ji}$ is the atomic number of the $j$ element in the $i$-th component molecule; $e$ is the total number of element species in the reaction system; $b_j$ is the amount of the j element. The calculation methods of reformate mole fraction and $H_2$ yield index are as follows:

$$y_i = \frac{n_i}{\sum_{i=1}^{N} n_i} \quad (4)$$
$$Y_{H_2} = \frac{n_{H_2}}{b_C} \quad (5)$$

$Y_{H_2}$ is the $H_2$ yield

## 3. SIMULATION RESULTS AND ANALYSIS

Temperature is an important parameter in ship SOFC-GT hybrid system, it will cause the diesel cracking gas to undergo a selective process. S/C (Ratio of $n_{H_2O}$ to $n_C$) is adjusted by changing the molar amount of $H_2O$ without changing the feed of diesel cracking gas. Changes in S/C cause equilibrium shifts that affect the product distribution of the reforming system. Low S/C will cause carbon deposition, and high S/C will increase the system humidity, dilute the fuel concentration, and increase energy consumption.

The thermodynamic parameters of the ship SOFC-GT hybrid system are from the previous research results of our research group[14,15]. During safe operation, the pressure change range is 1~4atm, and the temperature safety boundary is 1023~1223K. Under rated operating condition, S/C is 2, the fuel inlet temperature is 1023K,

and the SOFC operating pressure is 3.68bar. Among the researched variable working condition parameters in this paper, temperature ranges from 923 to 1123 K, S/C is 2~4, and pressure is 1~4 bar. Thermodynamic analysis of $H_2$ production from diesel cracking gas is carried out.

Table 2 shows the product distribution of diesel reforming under the rated operating conditions (T=1023K, S/C=2, P=3.68bar) of the ship SOFC-GT hybrid power system. The conversion rate of $C_1$-$C_4$ diesel cracking gas is close to 100%. The $H_2$ mole fraction in the product is close to 50%, and the $H_2$-rich fuel produced by the reaction can be used for the subsequent electrochemical reaction in the SOFC-GT hybrid system and can be fully utilized. However, there is still 6.9% carbon deposition, and S/C can be appropriately increased to suppress the generation of carbon deposition.

Table 2. Molar fraction of reforming products under rated operating condition

| Product | $CH_4$ | $C_2$-$C_4$ | $H_2$ | C | CO | $CO_2$ | $H_2O$ |
|---|---|---|---|---|---|---|---|
| Molar fraction (%) | 0.37 | 0 | 49.88 | 6.9 | 11.62 | 5.05 | 26.17 |

## 3.1 Influence of temperature and S/C on reformate

Fig. 1. shows the change of product mole fraction with temperature under rated conditions of S/C and pressure. When the temperature is above 900K. The mole fraction of $H_2$ in the product is above 40% and keeps rising, reaching 56% at 1123K. CO and $H_2$ show the same change trend, which confirm that the main reactions in the reaction system are steam reforming reaction R1-R6. The mole fractions of $H_2O$, $CO_2$, and $CH_4$ all decrease with increasing temperature. The $C_2$-$C_4$ small molecular hydrocarbons in the reaction products are completely converted, and the conversion rate of $CH_4$ also reaches 100% after 1023K. Carbon deposition is always present and decreases with increasing temperature. At 1123K, it is still 2.1%.
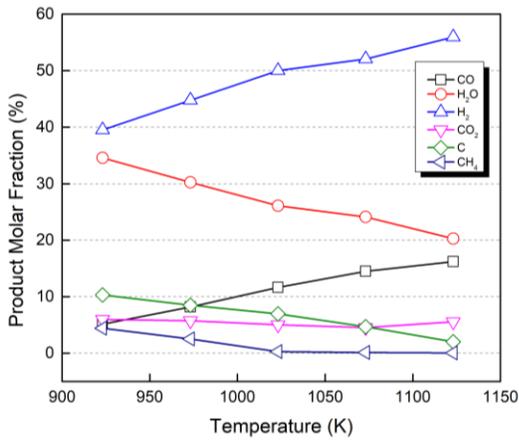
Fig. 1. Influence of temperature on product molar fraction

Fig. 2. shows the variation law of $H_2$ yield with temperature and S/C under rated pressure. It can be seen from the figure that the $H_2$ yield reaches the maximum value of 2.65 when the temperature is 1123K and S/C is 4. In the temperature range of 923-1123K, the $H_2$ yield increases with the increase of temperature and it is positively correlated with S/C. When the temperature is lower than 1020K, the angle between the contour line of the $H_2$ yield and the vertical axis is larger, indicating that the temperature has a greater influence on the $H_2$ yield. However, when the temperature is higher than 1020K, the $H_2$ yield is mainly affected by S /C.
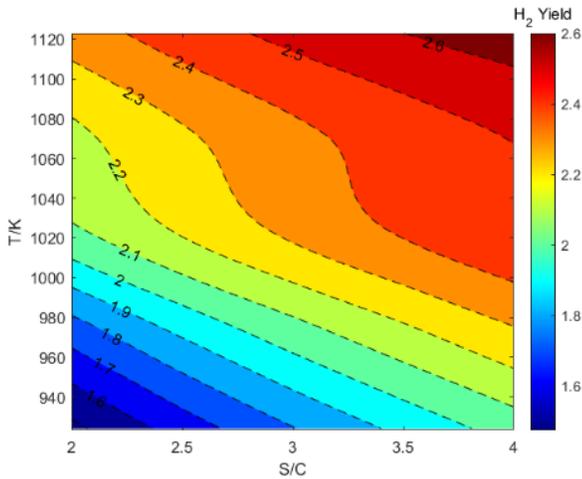


Fig. 2. Influence of temperature and S/C on $H_2$ yield
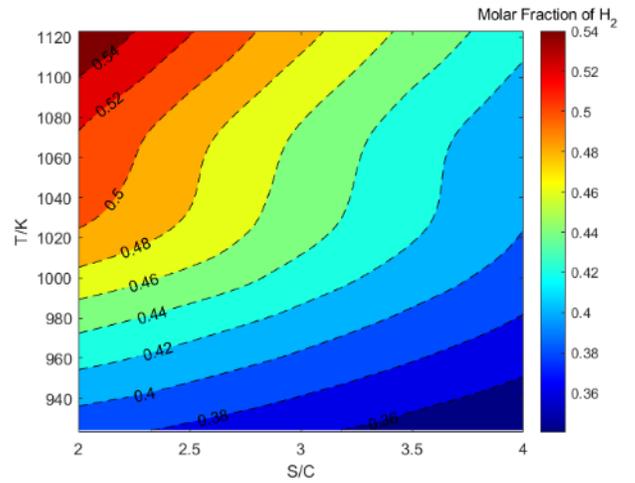


Fig. 3. Influence of temperature and S/C on $H_2$ molar fraction
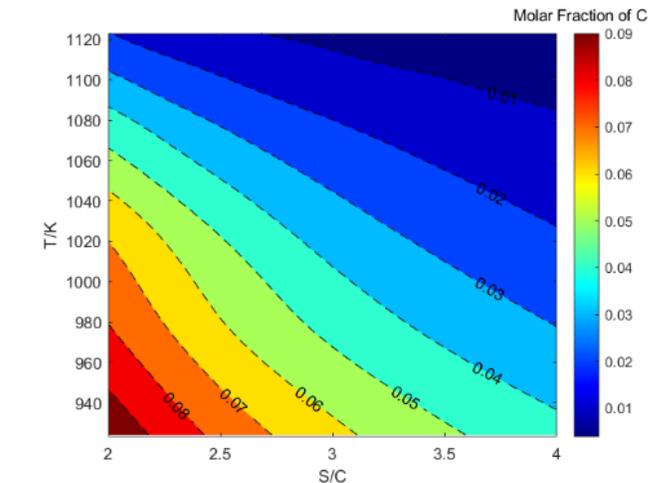


Fig. 4. Influence of temperature and S/C on carbon deposition

Fig. 3. shows the effect of $H_2$ mole fraction by temperature and S/C in equilibrium state. With the increase of S/C, the content of $H_2O$ increases significantly, which will dilute the $H_2$ in the products. When the temperature is above 1023K, the increase of the $H_2$ mole fraction with temperature increasing is not obvious, while the increase of S/C will still significantly dilute the $H_2$ content. The increase of S/C increases the $H_2$ yield, but reduces the $H_2$ mole fraction, so it is very important to choose a suitable value. From the figure, S/C is more suitable in the range of 2~3.

Fig. 4. shows the variation law of carbon deposition with temperature and S/C. It can be seen from the figure that the carbon deposition is mainly in the area below 980K and the S/C is below 2.5. Increasing the temperature and S/C can effectively inhibit the generation of carbon deposition. In summary the optimal reaction temperature is above 1000K, and the S/C is most suitable in the range of 2.5-3.

### 3.2 Influence of temperature and pressure on reformate

Fig. 5. shows the law of the effect of temperature and pressure on the $H_2$ yield. In the high temperature region above 1000K, the pressure has little effect on the $H_2$ yield. And below 1000K, the increase of pressure will lead to the decrease of $H_2$ yield. This is because the main reactions R1-R6 are all reactions of increasing volume, and the increase of pressure has an inhibitory effect on the steam reforming reaction. The same is true for the variation of $H_2$ mole fraction. Fig. 6 shows the variation of carbon deposition with temperature and pressure. The high temperature area above 1000K has less carbon deposition and is almost unaffected by pressure. The increase of pressure below 1000K has a little inhibitory effect on carbon deposition, and most of the carbon deposition reactions are volume reduction reactions. To sum up, when the reaction temperature is high enough, the effect of pressure change on reforming can be ignored, and more consideration should be given to the pressure requirements in the SOFC-GT hybrid system.
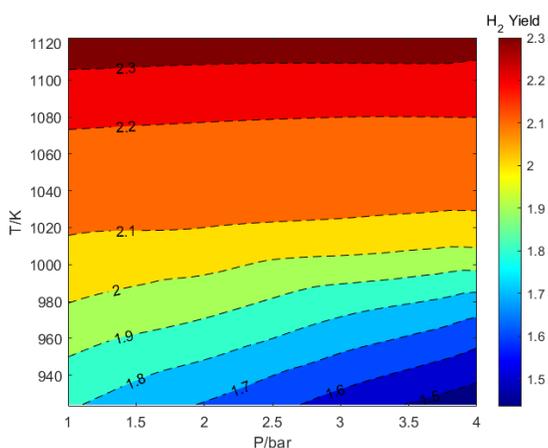


Fig. 5. Influence of temperature and pressure on $H_2$ yield
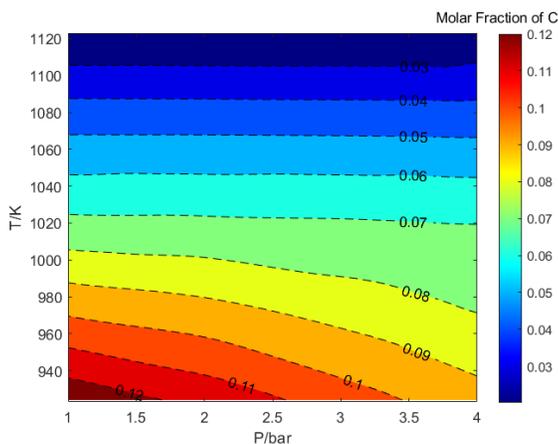


Fig. 6. Influence of temperature and pressure on carbon deposition

### 3.3 Analysis

It can be seen from Fig. 1 to 6 that temperature is the most important factor in diesel reforming reaction. Increasing the temperature can increase the $H_2$ yield and effectively reduce carbon deposition. Increasing the S/C can suppress carbon deposition and increase the $H_2$ yield, but it will also dilute the mole fraction of $H_2$ in the product. It is important to choose a reasonable S/C. The effect of pressure on the reaction at high temperature is negligible.

### 4. EXPERIMENTAL VERIFICATION OF $H_2$ PRODUCTION BY DIESEL REFORMING

In order to verify the accuracy of the reforming model, the corresponding marine diesel reforming experiments were carried out in this paper, and the errors between the experimental results and the simulated values under the rated operating conditions of the SOFC-GT hybrid system were compared.

### 4.1 Marine fuel preparation

Marine diesel oil (GB 19147-2016) was selected as the experimental raw material. In the chemical composition of the diesel oil, the mass fraction of saturated hydrocarbons is 65~85%, the mass fraction of aromatic hydrocarbons is 5%~30%, and the mass fraction of olefins is 0~5%. Among them, the H/C molar ratio of hydrocarbons is 1.8~2.3. And the carbon content is mainly distributed between $C_{10}$~$C_{20}$, among which, the content of $C_{16}$ is the highest. Table 4 shows the chemical composition obtained from the experimental analysis of marine diesel.

Table 4. Marine diesel chemical composition

| Composition | Weight fraction(%) |
|---|---|
| Saturated hydrocarbons | 74.1 |
| Paraffin | 58.2 |
| Naphthenic | 15.9 |
| Olefins | 4.4 |
| Aromatic hydrocarbons | 21.5 |
| Total | 100.0 |

### 4.2 Experimental test

Fig 7 shows a schematic diagram of the experimental setup of the entire reaction system. The experiment was divided into two parts, diesel cracking and cracking gas reforming. The reaction conditions of the diesel cracking experiment were fixed: the cracking temperature was 903K, the oil input was 0.5ml/min, and the pressure was 0.2MPa. The diesel oil was pumped into the preheater for heating, evaporated into diesel steam and then sent

to the cylindrical fixed bed reactor for cracking reaction. The middle part of the reactor was a catalyst layer, the catalyst was in powder form, and the upper and lower parts were sealed with quartz wool and quartz sand. The reaction product entered the gas-liquid separator for condensation, and the liquid product was collected in the conical flask, mainly $C_{5+}$ gasoline. The gaseous products were divided into two paths through the three-way valve, mainly $C_1 \sim C_4$ small molecular hydrocarbons. One path of the cracked gas was passed into a gas chromatograph (GC) for component analysis. And the other path of cracked gas was mixed with distilled water and preheated in the preheater, and both were passed

into the reformer in a gaseous state to participate in the subsequent reforming reaction. The temperature range of the cracking gas reforming experiment was 973-1073K, the intake gas volume was 20ml/min, and the water intake volume was 0.1-0.2ml/min. The reforming catalyst was long strip and fixed in the center of the cylindrical reactor, and the mixed gas underwent steam reforming reaction on the surface of the catalyst. The reaction product was filtered to remove water vapor through the condenser, and the obtained dry gas was analyzed by GC. The main components were $H_2$, CO, $CO_2$, and $CH_4$.
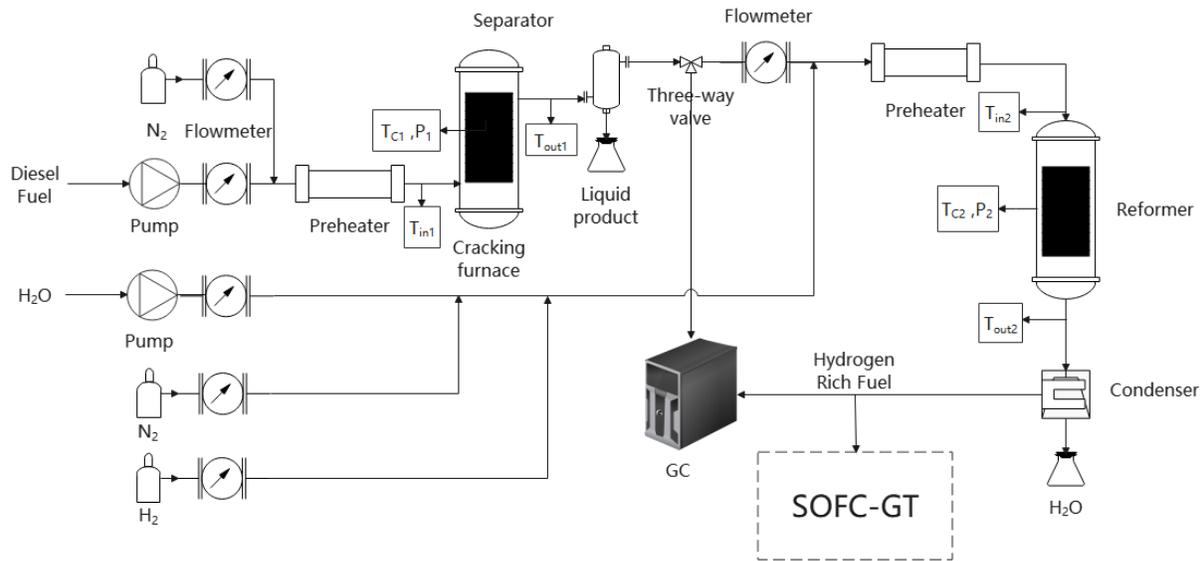


Fig. 7. Schematic diagram of diesel cracking-reforming reaction system

### 4.3  Experimental result

#### 4.3.1 Marine diesel cracking results

Fig. 8. is the result of testing the gas produced in the diesel cracking experiment in a gas chromatograph. The ordinate is the voltage signal, and the abscissa is the test time of the gas sample in the GC and the time when each component is detected. From left to right are the peak signals of $C_1 \sim C_4$. Table 5 and Table 6 are the experimental results of diesel catalytic cracking at 903K. From Table 5, the main components in the cracked gas are $C_1 \sim C_3$. When calculating S/C in subsequent reforming experiments, the cracked gas can be replaced by the average composition $C_{2.44}H_{6.09}$. Comparing Table 4 and Table 6, it can be seen that after diesel cracking, a large amount of saturated hydrocarbons are converted into olefins and aromatic hydrocarbons. It is mainly due to the chain scission of macromolecular chain hydrocarbons to generate small molecular hydrocarbons, and the remaining carbon chains generate 'C=C' and benzene

rings. There are still large carbon molecules in the lysate, so secondary cracking can be considered.
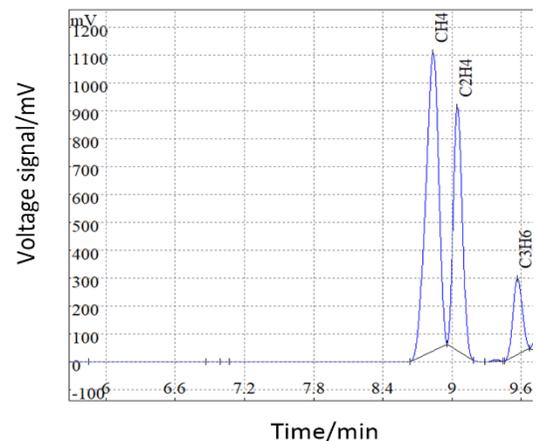


Fig. 8. GC peak graph of marine diesel cracking gas

Table 5 Molar fraction of marine diesel cracking gas

| Composition | $CH_4$ | $C_2H_{4+X}$ | $C_3H_{6+X}$ | $C_4H_{8+X}$ |
|---|---|---|---|---|
| Molar fraction (%) | 21.04 | 21.74 | 49.32 | 7.89 |

Table 6. Marine diesel lysate chemical composition

| Composition | Weight fraction (%) |
|---|---|
| Saturated hydrocarbons | 29.6 |
| Paraffin | 23.5 |
| Naphthenic | 6.1 |
| Olefins | 21.4 |
| Aromatic hydrocarbons | 49.0 |
| Total | 100.0 |

### 4.3.2 Marine diesel cracked gas reforming result

Marine diesel cracked gas reforming was carried out under the rated working conditions of ship SOFC-GT, that is, T=1023K, S/C=2, P=3.68bar. Fig. 9. shows the test result of the dry gas products (removal of water vapor and carbon deposits) in the gas chromatograph. Table 7 shows the comparison between the simulated data and experimental data of dry gas products under rated operating conditions. The absolute errors between the simulation results and the experimental results are all below 3%. In general, the reforming model can accurately predict the molar concentration of $H_2$ and the $H_2$ yield in the reformed product of diesel cracked gas.

Table7 Comparison of reformed dry gas products under rated conditions

| Composition | $H_2$ | $CH_4$ | CO | $CO_2$ |
|---|---|---|---|---|
| Simulation results (%) | 74.53 | 0.56 | 17.36 | 7.55 |
| Experimental results (%) | 71.84 | 1.89 | 17.05 | 9.22 |
| Absolute error (%) | 2.69 | 1.33 | 0.31 | 1.67 |
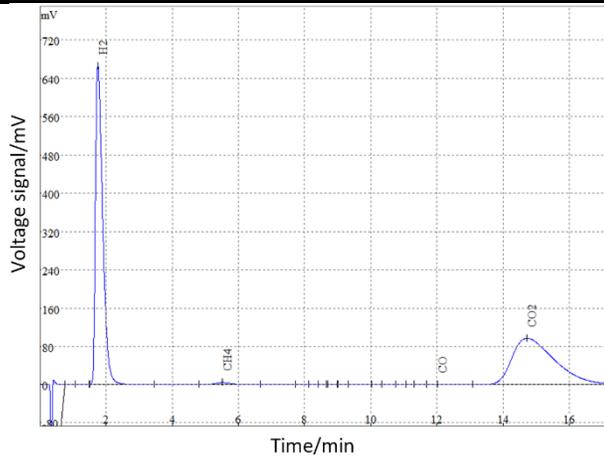


Fig. 9. GC peak graph of reforming dry gas products

### 4.3.3 Reforming catalyst carbon deposition analysis

After a stable reforming test for 20 hours, the surface morphology observation and elemental analysis of the marine diesel reformer were carried out by Scanning Electron Microscope-Energy Dispersive Spectrometer (SEM-EDS). Fig. 10 (a) is the scanning electron microscope image of the catalyst surface magnified by 500 times, and the line scanning path during the EDS energy spectrum analysis is marked in the figure. The catalyst shows a rough surface morphology. The bright white part in the figure represents noble metal catalysts such as Pt, and the black part represents the carbon deposits generated on the surface of the catalyst.



(a)　　　　　　　　　　(b)
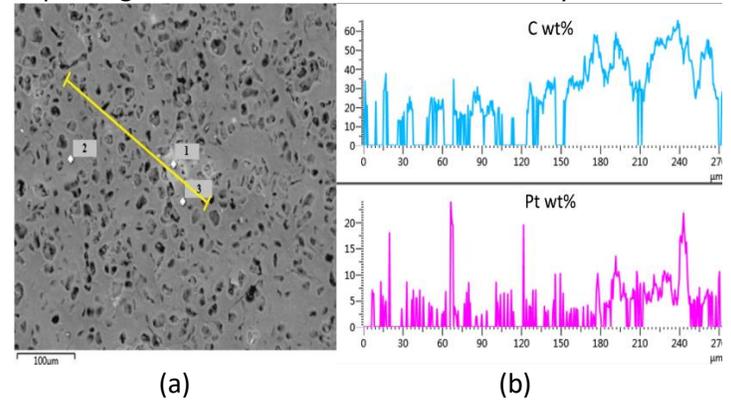
Fig. 10. SEM image of catalyst and EDS line scan results

Fig 10 (b) shows the main element content of the EDS line scan. It can be seen from the figure that the mass fraction of C element begins to increase after 120 microns, and the continuity is stronger, reaching more than 60% near 240 microns. In the vicinity of the position where the Pt element content reaches its peak, the carbon deposition content also increases significantly.

Table 8 shows the mass distribution results of each main element by EDS surface scanning before and after the catalyst reaction. After the reaction, the mass fraction of Pt element on the catalyst surface was 2.71%, while the mass fraction of C element reached 23.09%. It can be seen that no C element was detected in the catalyst that did not participate in the reaction, and only O, Al and Pt were detected for the main elements, which confirmed that the C element on the catalyst surface was generated by the carbon deposition reaction. This is consistent with the consistent presence of carbon deposits in the simulation results of Fig. 1. The carbon deposition reaction not only changes the surface morphology of the catalyst, but also affects the reforming performance of the catalyst.

Table 8 EDS analysis results of the main elements of the catalyst

| Reaction time | Unit | C | O | Al | Fe | Pt |
|---|---|---|---|---|---|---|
| 20h | wt% | 23.09 | 39.83 | 33.84 | 0.41 | 2.71 |
| 0 | wt% | 0 | 50 | 42.11 | 0.43 | 7.46 |

## 5. CONCLUSION

In this paper, under the operating conditions of ship SOFC-GT hybrid power system, the effects of temperature, S/C and pressure changes on $H_2$ yield and product distribution in marine diesel heterogeneous chemical reforming system were studied. And the results

were verified by marine diesel cracking-reforming experiments. The results can provide basic technical support for the safe and efficient operation of SOFC-GT hybrid system on ships and the continuous supply of ship fuel. The conclusions are as follows:

1) The temperature plays a decisive role in marine diesel reforming process. In the range of 923-1123K, the temperature increasement brings the $H_2$ yield and the $H_2$ mole fraction in the product to increase, and the carbon deposition decreases. The $H_2$ mole fraction can be up to 56%. The increase in pressure can slightly inhibit the generation of carbon deposition, but it will reduce the $H_2$ yield and $H_2$ mole fraction. But when the temperature is higher than 1000K, the effect of pressure is negligible.

2) The increase of S/C can increase the $H_2$ yield and inhibit the generation of carbon deposition. But a large increase in water vapor dilutes the mole fraction of $H_2$ in the product. Taken together, the optimal S/C is 2.5~3.

3) Under rated operating conditions, the $C_1$-$C_4$ small molecular hydrocarbons in the diesel cracking gas are completely converted to $H_2$, CO and $CO_2$. The $H_2$ mole fraction accounts for 50%, and the produced $H_2$-rich fuel can be used for the electrochemical reaction of SOFC in the subsequent hybrid system, which can be fully utilized.

## REFERENCE

[1] Olmer, N.; Comer, B.; Roy, B.; Mao, X.; Rutherford, D. Greenhouse Gas Emission from Global Shipping 2013–2015, Detailed Methodology[C]. The International Council on Clean Transportation: Washington, DC, USA, 2017.

[2] Joung, Tae-Hwan, Seong-Gil Kang, Jong-Kap Lee, and Junkeon Ahn. The IMO Initial Strategy for Reducing Greenhouse Gas (GHG) Emissions, and Its Follow-up Actions towards 2050[J]. Journal of International Maritime Safety, Environmental Affairs, and Shipping 4.1 (2020): 1-7.

[3] Joung, T. H. Initial IMO Strategy on Reduction of GHG Emissions from Ships and Its Follow-up Actions[C]. Europe-Korea Conference on Science and technology (EKC) 2019, Austria.

[4] IMO(MEPC74). 2019a. MEPC 74-WP.6 - Report of the fifth meeting of the Intersessional Working Group on Reduction of GHG emission.

[5] Azizi M A, Brouwer J. Progress in solid oxide fuel cell-gas turbine hybrid power systems: system design and analysis, transient operation, controls and optimization [J]. Applied Energy. 2018, 215:237-289.

[6] Baldi F, Moret S, Tammi K. The role of solid oxide fuel cells in future ship energy systems[J]. Energy. 2020, 194:116811.

[7] Inal M B, Deniz C. Assessment of fuel cell types for ships: Based on multi-criteria decision analysis[J]. Journal of Cleaner Production. 2020, 265:121734.

[8] U.S. Maritime Administration Workshop on Maritime Energy and Clean Emissions 29-30 January 2002. The St. Regis Washington, DC.

[9] Sun J, Stebe J, Kennell C. Feasibility and Design Implications of Fuel Cell Power for Sealift Ships[J]. Naval Engineers Journal. 2010, 122(3):87-102.

[10] Gerardo Valadez Huerta, Johanan Álvarez Jordán, Michael Dragon, Keno Leites, Stephan Kabelac. Exergy analysis of the diesel pre-reforming solid oxide fuel cell system with anode off-gas recycling in the SchIBZ project. Part I: Modeling and validation[J]. International Journal of Hydrogen Energy,2018,43:16684-16693.

[11] Sohyun Jeong, Daewook Kim, Jay H. Lee. Modeling and Simulation of Autothermal Reforming Reactor of Diesel over Ni-based Catalyst in Solid Oxide Fuel Cell based Auxiliary Power Unit System[J]. Computer Aided Chemical Engineering,2018,44:613-618.

[12] Fawad Rahim Malik, Zhang Tieqing, Young-Bae Kim. Temperature and Hydrogen flow rate controls of diesel autothermal reformer for 3.6 kW PEM fuel cell system with autoignition delay time analysis[J]. International Journal of Hydrogen Energy,2020,45:29345-29355.

[13] Remzi Can Samsun, Matthias Prawitz, Andreas Tschauder, Joachim Pasel, Ralf Peters, Detlef Stolten. An autothermal reforming system for diesel and jet fuel with quick start-up capability[J]. International Journal of Hydrogen Energy,2019,44:27749-27764.

[14] X Wang, X Mi, X Lv, Y Weng. Design and simulation of LNG-fueled SOFC-GT Hybrid System for ship application [C]. The 13th International Conference on Applied Energy. Nov. 29 - Dec. 5, 2021.

[15] X Wang, X Lv, X Mi, C Spataru, Y Weng. Coordinated Control Approach for Load following Operation of SOFC-GT Hybrid System[J]. Energy.2022,248.